International Conference on Applied Energy 2019
Aug 12-15, 2019, Västerås, Sweden
Paper ID: 912

EFFECTIVE DAMPING RATIO EXTRACTION FOR DELAYED FREQUENCY REGULATION SYSTEMS BASED ON SOLUTION OPERATOR TRANSFORMATION

Zhang Yimei[1], Dong Chaoyu[1*], Xiao Qian[1], Gao Qingbin[2], Jia Hongjie[1]
1 School of Electrical and Information Engineering, Tianjin University, Tianjin, China
2 Department of Mechanical Engineering, University of Alabama

ABSTRACT

The renewable power systems have become more susceptible to the system insecure than traditional power systems due to the reducing inertia and damping properties. In the meantime, inevitable time delays commonly exist in different procedures of the energy systems, such as computational delay, which may lead to poor performance, or even instability. Therefore, the time-delay impacts should be properly taken into account. However, the time-delay system belongs to the class of functional differential equations mathematically. With a transcendental characteristic equation, infinite dimension will increases transformation complexity and computation pressure.

To rapidly describe the time-delay impact for multi-area power systems with time delays, a dimension reduction method based on the solution operator discretization is proposed in this paper. The quantitative relationship between time delays and system damping ratio is revealed for the first time. It starts with a state space equation for the entire frequency regulation system, the spectrum of time delayed systems is transferred into the spectrum of infinite-dimensional operators, followed by discretizing the solution operator. After that, a simple approximate matrix of finite dimensions is established, which sufficiently reflects the effect of time delays. The proposed method can not only ensure low computational burden efficiency via dimension reduction, but also extract the nonlinear coupling between the time delay and the damping deterioration.

Keywords: renewable energy resources, dimension reduction, time delays, solution operator discretization.

1. INTRODUCTION

Nowadays, renewable energy sources (RESs) are attracting increasing attention as a solution to the problem of energy shortage. Traditional generations are being replaced by a large amount of RESs (e.g. wind and solar energy)[1]. The traditional synchronous generators (SGs) stored kinetic energy in their rotating mass and so they can provide inertia to the system. Also, they provide damping property for the grid through mechanical friction and electrical losses. However, short of rotating mass, the inertia of renewable power systems significantly falls. With increasing the penetration level of RESs into the grid, the influence of low inertia and damping on the dynamic system performance and stability increases, which induces frequency fluctuation. Therefore, the frequency control may be difficult in case of mismatch between electric power generation and load demand, with growing RESs penetration.

On the other side, with the continuous expansion of the power grid and the continuous developing in electrical loads[2], the interconnection among different power systems is strengthened. More and more time delays are penetrating into power systems, including the measurement and control loop, which leads to the appearance of the oscillations problems[3]. Identification of oscillation frequency, damping ratio, oscillation mode, and other parameters play a vital role in the management of dynamic characteristics, the subsequent control, and the secure operation of the system. Therefore, a characteristics and damping ratio extraction method is important for further analysis and controller design. However, most methods assume that time delays are negligible[4]. Obviously, these are inaccurate and will cause errors in the stability analysis and controller design. Some researches have modeled time delay as an exponential Laplace delay operator, the transcendental terms would be induced into the system characteristic equation, causing infinite dimensionality. Therefore, it is extremely difficult to directly solve this equation and analyze the system. Besides, the existence of multiple delays may increase the transformation complexity and computation pressure. To solve these problems, an effective damping ratio extraction method based on the solution operator transformation for delayed frequency regulation systems is proposed in this paper. A simple approximate matrix based on the solution operator is structured. According to the Spectral Mapping Principle, the eigenvalues and the corresponding eigenvectors of the delayed system can be obtained by computing the nonzero eigenvalues of the approximate matrix, which reflects the damping ratio, oscillation frequency of the system and the correlation of state variables. These reveal the qualitative and quantitative information of system modes, which can also be combined with various algorithms for stability analysis and controller design. Meanwhile, the dimension of the time-delay model is significantly reduced ensuring low computational burden and high effectiveness.

2. SYSTEM MODELING

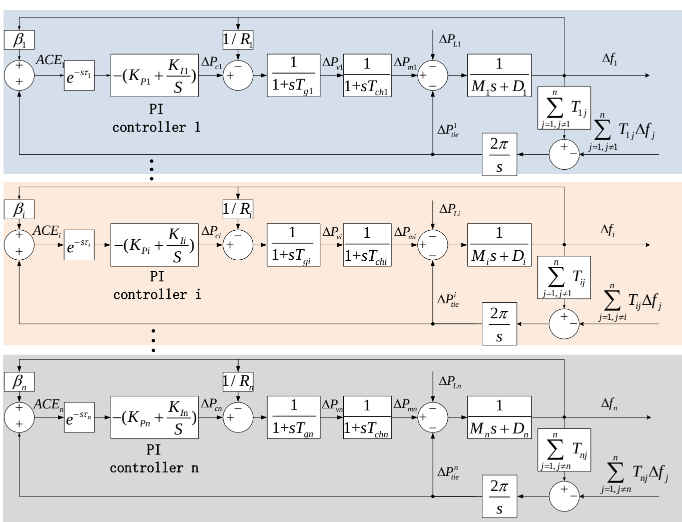

Fig 1 Dynamic model of multi-area LFC scheme.

For a multi-area load frequency control (LFC) scheme, as shown in Fig 1, all generation units in each control area are simplified as an equivalent generation unit. For area *i*, the dynamics are described as

$$\Delta\dot{P}_{m_i} = -\frac{1}{T_{ch_i}}\Delta P_{m_i} + \frac{1}{T_{ch_i}}\Delta P_{v_i} \tag{1}$$

$$\Delta\dot{P}_{v_i} = -\frac{1}{R_i T_{g_i}}\Delta f_i - \frac{1}{T_{g_i}}\Delta P_{v_i} + \frac{1}{T_{g_i}}\Delta P_{c_i} \tag{2}$$

$$\Delta\dot{f}_i = -\frac{D_i}{M_i}\Delta f_i + \frac{1}{M_i}\Delta P_{m_i} - \frac{1}{M_i}\Delta P^i_{tie} - \frac{1}{M_i}\Delta P_{L_i} \tag{3}$$

$$\Delta\dot{P}^i_{tie} = \sum_{j=1,\, j\neq i}^{n} 2\pi T_{ij}(\Delta f_i - \Delta f_j) \tag{4}$$

where ΔP_{m_i} , ΔP_{v_i} , Δf_i , ΔP_{L_i} are the deviations of the generator mechanical output, turbine valve position, frequency, and load respectively. ΔP_{c_i} is load reference set-point, ΔP^i_{tie} is the net exchange of tie-line power of the *i*th control area, M_i is the inertia of generator *i*; D_i is damping coefficient of generator *i*; T_{g_i} is time constant of governor *i*; T_{ch_i} is time constant of turbine *i*; T_{ij} is synchronizing power coefficient; R_i is speed droop coefficient.

The area control error *ACEᵢ* in a multi-area LFC is defined as

$$ACE_i = \beta_i \Delta f_i + \Delta P_{\mathrm{tie}_i} \tag{5}$$

For each area, the dispatch center is designed as

$$u_i(t) = -K_{pi}ACE_i - K_{Ii}\int ACE_i \tag{6}$$

Based on the dynamic equation above, the state-space model for the *i*th control area can be obtained

$$\begin{cases} \dot{\boldsymbol{x}}_i = \boldsymbol{A}_i\boldsymbol{x}_i + \boldsymbol{B}_i u_i + \sum\limits_{j=1,\, j\neq i}^{n} \boldsymbol{A}_{ij}\boldsymbol{x}_j + \boldsymbol{F}_i \Delta P_{L_i} \\ \boldsymbol{y}_i = \boldsymbol{C}_i \boldsymbol{x}_i \end{cases} \tag{7}$$

where

$$\boldsymbol{x}_i = \begin{bmatrix} \Delta f_i & \Delta P_{m_i} & \Delta P_{v_i} & \int ACE_i & \Delta P^i_{tie} \end{bmatrix}^T \quad u_i = \Delta P_{c_i} \tag{8}$$

$$\boldsymbol{A}_i = \begin{bmatrix} -D_i/M_i & 1/M_i & 0 & 0 & -1/M_i \\ 0 & -1/T_{ch_i} & 1/T_{ch_i} & 0 & 0 \\ -1/R_i/T_{g_i} & 0 & -1/T_{g_i} & 0 & 0 \\ \beta_i & 0 & 0 & 0 & 1 \\ \sum\limits_{j=1,\, j\neq i}^{n} 2\pi T_{ij} & 0 & 0 & 0 & 0 \end{bmatrix} \tag{9}$$

$$\boldsymbol{C}_i = \begin{bmatrix} \beta_i & 0 & 0 & 0 & 1 \\ 0 & 0 & 0 & 1 & 0 \end{bmatrix} \tag{10}$$

$$\boldsymbol{A}_{ij} = \begin{bmatrix} 0 & 0 & 0 & 0 & 0 \\ 0 & 0 & 0 & 0 & 0 \\ 0 & 0 & 0 & 0 & 0 \\ 0 & 0 & 0 & 0 & 0 \\ -2\pi T_{ij} & 0 & 0 & 0 & 0 \end{bmatrix} \tag{11}$$

$$\boldsymbol{B}_i = \begin{bmatrix} 0 & 0 & 1/T_{g_i} & 0 & 0 \end{bmatrix}^T \tag{12}$$

$$F_i = \begin{bmatrix} -1/M_i & 0 & 0 & 0 & 0 \end{bmatrix}^T \tag{13}$$

The time-delay model of the multi-area power system can be described by following delayed differential equations.

$$\begin{cases} \dot{\boldsymbol{x}}(t) = \tilde{\boldsymbol{A}}\boldsymbol{x}(t) + \tilde{\boldsymbol{A}}_d \boldsymbol{x}(t-\tau), t \geq 0 \\ x(t) = \Delta x_0 \triangleq \varphi, t \in \left[-\tau_{\max}, 0\right] \end{cases} \tag{14}$$

where φ is the initial system state.

$$\boldsymbol{x} = \begin{bmatrix} \boldsymbol{x}_1^T & \boldsymbol{x}_2^T & \cdots & \boldsymbol{x}_n^T \end{bmatrix}^T \tag{15}$$

$$\Delta \boldsymbol{P}_L = \begin{bmatrix} \Delta P_{L_1} & \Delta P_{L_2} & \cdots & \Delta P_{L_n} \end{bmatrix}^T \tag{16}$$

$$\tilde{\boldsymbol{A}} = \begin{bmatrix} \boldsymbol{A}_1 & \boldsymbol{A}_{12} & \cdots & \boldsymbol{A}_{1n} \\ \boldsymbol{A}_{21} & \boldsymbol{A}_2 & \cdots & \boldsymbol{A}_{2n} \\ \vdots & \vdots & \ddots & \vdots \\ \boldsymbol{A}_{n1} & \boldsymbol{A}_{n2} & \cdots & \boldsymbol{A}_n \end{bmatrix} \tag{17}$$

$$\tilde{\boldsymbol{A}}_d = -\boldsymbol{BKC} \quad \boldsymbol{B} = diag\left\{\boldsymbol{B}_1 \cdots \boldsymbol{B}_n\right\} \tag{18}$$

$$\boldsymbol{K} = diag\left\{\boldsymbol{K}_1 \cdots \boldsymbol{K}_n\right\} \quad \boldsymbol{C} = diag\left\{\boldsymbol{C}_1 \cdots \boldsymbol{C}_n\right\} \tag{19}$$

The characteristic equation of (14) the system is

$$(\tilde{\boldsymbol{A}} + \tilde{\boldsymbol{A}}_d e^{-\lambda \tau_i})v = \lambda v \tag{20}$$

where λ is an eigenvalue and v is the corresponding eigenvector.

3. SOLUTION OPERATOR-BASED METHOD

In order to avoid directly solving equations (20), the spectrum of time delayed systems is transformed into the spectrum of the solution operator first. The operator is then discretized, resulting in a finite-dimensional discretization matrix. The minimum damping ratio and the dominant oscillation frequency of the time-delay power system can be rapidly derived from the matrix.

The details of the theoretical foundation of the extraction method are as follows.

3.1 Theoretical foundation

The solution operator *T*(*h*) maps the initial condition φ at *t* into the system state at *t* + *h*, where *h* is the transfer step length satisfying $0 \leq h \leq \tau_{\max}$

$$(\boldsymbol{T}(h)\boldsymbol{\varphi})(t) = \Delta \boldsymbol{x}_h(t) = \Delta \boldsymbol{x}(t+h) \tag{21}$$

Eigenvalues μ of *T*(*h*) can be obtained from eigenvalues λ of multi-area LFC

$$\mu = e^{\lambda h}, \quad \mu \in \sigma(\boldsymbol{T}(h)) \setminus \{0\} \tag{22}$$

$\sigma(\cdot)$ denotes the spectrum of an operator or a matrix. \ denotes the operation of set difference. The eigenvalues in *s*-plane are then transformed into eigenvalues of *T*(*h*) in the *z*-plane.

3.2 Solution operator discretization scheme

The rightmost eigenvalues λ with the largest real parts of systems can be recovered from μ with maximum moduli.

The problem is transformed into computing μ from *T*(*h*), which is an infinite-dimensional problem. To reduce the complexity, the operator *T*(*h*) could be discretized by implicit Runge-Kutta methods first. The eigenvalues can then be computed from the resultant finite-dimensional discretized matrix.

First, the *N* sub-intervals of length *h* are discretized by the abscissae of a *p*-order *s*-stage implicit Runge-Kutta method, resulting in a set of discrete points.

According to (21), ***T***(*h*) has two segments:

1) Time Integration: when $t \in \left[-h, 0\right]$, $\Delta \boldsymbol{x}(t)$ can be computed from the following equation by p-order *s*-stage implicit Runge-Kutta method:

$$\Delta \dot{\boldsymbol{x}}_h(t) = \tilde{\boldsymbol{A}} \Delta \boldsymbol{x}_h(t) + \tilde{\boldsymbol{A}}_d \Delta \boldsymbol{x}_h(t-\tau_i) \tag{23}$$

2) Shift: For $t \in \left[-\tau_{\max}, -h\right]$, ***T***(*h*) is a shift, $\Delta \boldsymbol{x}_h(t)$ is always the initial condition part.

In summary, ***T***(*h*) can be reformulated as follows.

$$\Delta \boldsymbol{x}_h(t) = \begin{cases} \varphi(0) + \int_0^t (\tilde{\boldsymbol{A}} \Delta \boldsymbol{x}_h(s) + \tilde{\boldsymbol{A}}_d \Delta \boldsymbol{x}_h(s-\tau_i)) \, \mathrm{d}\, s, t \in \left[-h, 0\right] \\ \varphi(t+h), t \in \left[-\tau_{\max}, -h\right] \end{cases} \tag{24}$$

By applying IRK and using the shift property to assess system states at the points of Ω_{Ns}, the approximate matrix $\boldsymbol{T}_{Ns}$ to ***T***(*h*) is obtained.

$$\boldsymbol{T}_{Ns} = \begin{bmatrix} \boldsymbol{R}_{Ns}^{-1} \boldsymbol{\Sigma}_{Ns} \\ \boldsymbol{\Gamma}_{Ns} \end{bmatrix} \quad \boldsymbol{\Gamma}_{Ns} = \begin{bmatrix} \boldsymbol{I}_{(N-1)sn} \\ \boldsymbol{0}_{(N-1)sn \times sn} \end{bmatrix} \tag{25}$$

$$\begin{cases} \boldsymbol{R}_{Ns} = \boldsymbol{I}_{sn} - h\boldsymbol{A} \otimes \tilde{\boldsymbol{A}} \\ \boldsymbol{\Sigma}_{Ns} = \boldsymbol{L}_0^T \otimes \boldsymbol{I}_n + h(\boldsymbol{A}\boldsymbol{L}_1^T) \otimes \tilde{\boldsymbol{A}}_d \end{cases} \tag{26}$$

where $\boldsymbol{A} \in \mathbf{R}^{s \times s}$ is formed of elements in the Butcher's tableau, $\boldsymbol{L}_1 \in \mathbf{R}^{Ns \times s}$ are constant Lagrange interpolation matrices.

Then, both system characteristics and time delays can be reflected in the finite-dimensional approximate matrices to ***T***(*h*), i.e., $\boldsymbol{T}_{Ns}$.

4. SPACE TRANSFORMATION

To improve computing efficiency, a space conversion technique is presented to shift the desirable eigenvalues so that they become dominant in moduli.

Eigenvalues λ are first rotated by $\theta(=\arcsin(\zeta))$ in counterclockwise direction, which is then amplified by α times to increase the relative distance between them.

$$\mu' = e^{\lambda' h} \quad \lambda' = \alpha e^{-j\theta} \lambda \tag{27}$$

After space transformation, the discretized matrix of the solution operator $\boldsymbol{T}_{Ns}$ turns to $\boldsymbol{T}_{N's}$

$$\boldsymbol{T}_{N's} = \begin{bmatrix} \boldsymbol{R}_{N's}^{-1}\boldsymbol{\Sigma}_{N's} \\ \boldsymbol{\Gamma}_{N's} \end{bmatrix} \tag{28}$$

where

$$\begin{cases} \boldsymbol{R}_{N's} = \boldsymbol{I}_{sn} - h\boldsymbol{A} \otimes \tilde{\boldsymbol{A}}_0{}' \\ \boldsymbol{\Sigma}_{Ns} = \boldsymbol{L}_0^T \otimes \boldsymbol{I}_n + h(\boldsymbol{A}\boldsymbol{L}_1^T) \otimes \tilde{\boldsymbol{A}}_d{}' \end{cases} \tag{29}$$

5. KRYLOV SUBSPACE DIMENSION REDUCTION

The discretized matrix after system space transformation contains the parameters of oscillation frequency, damping ratio, and oscillation mode. And simplification from infinite dimension to finite dimension is realized, but the dimension of the matrix $\boldsymbol{T}_{N's}$ is still large. Therefore, it is necessary to obtain a reduced-dimension matrix that retains the important properties of the original system. A structure-preserving reduction algorithm is presented based on a Krylov subspace.

The algorithm is developed under the framework of projection. We use a second-order Krylov subspace as the projection subspace. Subsequently, an Arnoldi method is used to generate an orthonormal basis $\boldsymbol{V}_m$ of the projection subspace as follows:

$$\begin{aligned} \boldsymbol{T}_{N's}\boldsymbol{V}_m &= \boldsymbol{V}_m\boldsymbol{H}_m + h_{m+1,m}v_{m+1}e_m^T \\ &= \boldsymbol{V}_m\boldsymbol{H}_m + f_m e_m^T \\ &= \boldsymbol{V}_{m+1}\tilde{\boldsymbol{H}}_m \end{aligned} \tag{30}$$

where $\boldsymbol{H}_m, \tilde{\boldsymbol{H}}_m$ are *m*-order and *m*×*m*-order upper Hessenberg matrix respectively. If f_m is small enough, the eigenvalues of $\boldsymbol{H}_m$ will approach the eigenvalues of matrix $\boldsymbol{T}_{N's}$ infinitely. So the eigenvalue of $\boldsymbol{H}_m$ is used as the approximate eigenvalue of $\boldsymbol{T}_{N's}$.

The resulting reduced matrix $\boldsymbol{H}_m$ not only preserves the structure but also reduces the dimensions.

6. DAMPING RATIO EXTRACTION

In actual systems, the critical electromechanical oscillation modes determine the system stability. The corresponding minimum damping ratio and dominant oscillation frequency are what we really care about, which can be obtained by calculating the critical eigenvalue of reduced-dimension matrix $\boldsymbol{H}_m$.

The eigenvalue is usually expressed as a conjugate pair of $\lambda = \sigma \pm j\omega$. When the real part is positive, the oscillation of the system will increase. When the real part is negative, the dynamic mode of the system is an attenuation oscillation. The oscillation frequency is determined by the imaginary part of the eigenvalue, and the magnitude is $f = \omega / 2\pi$. The minimum damping ratio is determined by the real part of eigenvalue, and the value is

$$\xi = -\sigma / \sqrt{\sigma^2 + \omega^2} \tag{31}$$

When $\xi < 0$, it is an unstable oscillation mode; when $\xi = 0$, it is a critical stable oscillation mode; when $\xi > 0$, it is a stable oscillation mode. The larger damping ratio indicates a more stable system.

7. CASE STUDY I: TWO-AREA LFC SCHEME

Case studies are carried out based on a two-area LFC scheme first. Parameters are tabulated in [5], [6]. The dominant oscillation frequency and the minimum damping ratio of each LFC scheme with respect to gains of the PI controller (K_P, K_I) are calculated based on the extraction method proposed.

First, the relationship between time delay and system damping are summarized in Fig 2 and Fig 3, respectively. It can be found that, with the increase of the time delay τ, the dominant oscillation frequency f increases first and then decreases, while the minimum damping ratio stays the same first and then significantly decreases. And the changing curves both have tipping points, which are different with respect to the different gains of PI controllers. It is also shown that a relatively larger minimum damping ratio ξ can be obtained under smaller K_P and K_I, and ξ is reduced sharply for bigger K_P and K_I. Small changes in K_p may cause a significant change of f and ξ. When K_p increases to a certain extent, the mutation occurs for both f and ξ.

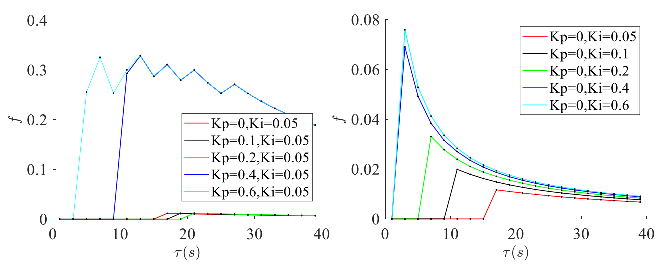

Fig 2 Dominant oscillation frequency $f \propto \tau$ (two-area LFC)

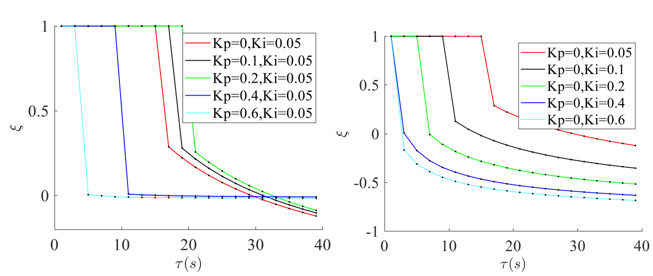

Fig 3 Minimum damping ratio $\xi \propto \tau$ (two-area LFC)

Thus, (K_P,K_I) should be properly chosen to have a larger minimum damping ratio and a smaller dominant oscillation frequency with a relatively small degradation of the dynamic performance. During the design and tuning of the controller, a trade-off between the delay margin and dynamic performance can be achieved.

Table I. Minimum damping ratio $\xi \propto (K_P,K_I)$
(two-area LFC τ=20s)

ξ	K_I						
K_p	0.05	0.1	0.15	0.2	0.4	0.6	1
0	0.194	-0.136	-0.278	-0.362	-0.522	-0.593	-0.665
0.05	0.221	-0.127	-0.273	-0.359	-0.521	-0.592	-0.664
0.1	0.247	-0.119	-0.269	-0.357	-0.520	-0.592	-0.664
0.2	1.000	-0.104	-0.262	-0.352	-0.518	-0.591	-0.664
0.4	-0.002	-0.088	-0.252	-0.344	-0.515	-0.589	-0.663
0.6	-0.011	-0.012	-0.247	-0.341	-0.513	-0.588	-0.662
1	-0.024	-0.024	-0.024	-0.024	-0.512	-0.586	-0.661

Table II. Minimum damping ratio $\xi \propto (K_P,K_I)$
(two-area LFC τ=5s)

ξ	K_I						
K_p	0.050	0.100	0.150	0.200	0.400	0.600	1.000
0.0	1.000	1.000	1.000	1.000	-0.172	-0.309	-0.439
0.05	1.000	1.000	1.000	1.000	-0.164	-0.305	-0.437
0.1	1.000	1.000	1.000	1.000	-0.157	-0.301	-0.435
0.2	1.000	1.000	1.000	1.000	-0.145	-0.295	-0.432
0.4	1.000	1.000	1.000	1.000	-0.131	-0.286	-0.427
0.6	0.005	0.005	0.004	0.004	-0.135	-0.283	0.424
1	-0.045	-0.046	-0.046	-0.047	-0.186	-0.296	-0.424

And simulation studies are used to verify the effectiveness and accuracy of the proposed method. The delay margin (K_P=0.05,K_I=0.05) calculated by the proposed method is 31s (the simulation step is 2s). By comparing with simulation, which is coincident with simulations in Fig 4, Fig 5. The result also shows that time delay causes the whole system oscillation due to the damping loss.

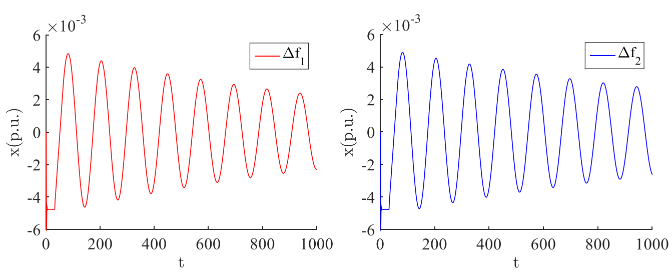

Fig 4 Frequency variation (K_P=0.05,K_I =0.05) with τ=30s

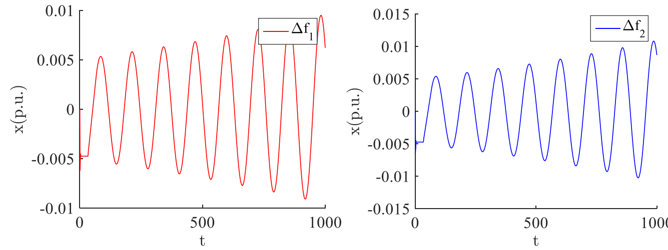

Fig 5 Frequency variation (K_P=0.05,K_I =0.05) with τ=32s

8. CASE STUDY II: THREE-AREA LFC SCHEME

Similar calculations are carried out for a three-area LFC system. K_P and K_I are changed simultaneously obtaining results in Fig 6 and Fig 7. The anti-damping effect of time delay is shown in Fig 8.

The results show that the gain of the PI controller is one of the key factors affecting the minimum damping ratio and dominant oscillation frequency. Changing the gain in a certain range has no substantial influence of f and ξ . But if the gain is increased above the range, a small change may lead to a significant change of f , ξ . With the same parameters, the increase of the time delay will decrease the minimum damping ratio.

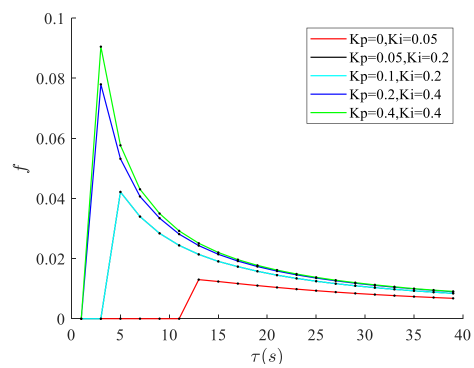

Fig 6 Dominant oscillation frequency $f \propto \tau$ (three-area LFC)

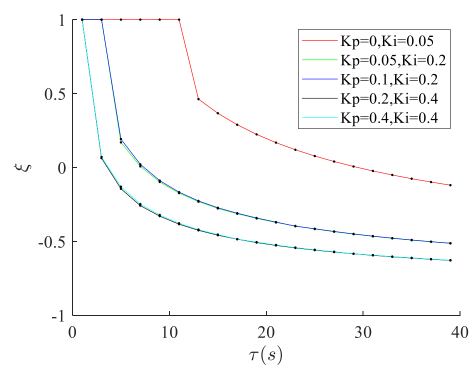

Fig 7 Minimum damping ratio $\xi \propto \tau$ (three-area LFC)

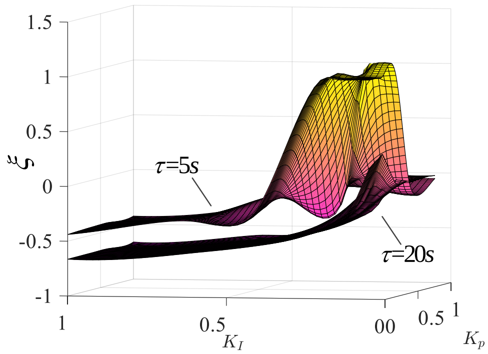

Fig 8 Minimum damping ratio $\xi \propto (K_P,K_I)$

9. CONCLUSIONS

In this paper, an effective damping ratio extraction method based on solution operator transformation is presented for frequency regulation systems considering time delays. The contributions are summarized as below:

First, the dimension reduction of the model with time delay is realized through solution operator transformation, which ensures high efficiency.

Second, the coupling of controller and time delay is revealed influencing the dominant oscillation frequency and the minimum damping ratio. Due to the time delay, ξ is reduced sharply for bigger K_P and K_I. A small increment of the controller gains may lead to a significant decrement of the damping ratio.

Third, the time-delay impact is imposed with low-frequency oscillation and damping loss causing the system instability.

REFERENCE

[1] S. Ghavidel, A. Rajabi, M. J. Ghadi, A. Azizivahed, L. Li, J. F. Zhang. Risk-constrained demand response and wind energy systems integration to handle stochastic nature and wind power outage [J]. IET Energy Systems Integration, 2019, 1(2): 114-120.

[2] C. Y. Dong, H. J. Jia, Q. W. Xu, et al. Time-delay stability analysis for hybrid energy storage system with hierarchical control in dc microgrids[J]. IEEE Transactions on Smart Grid, 2017, 9(6): 1-1.

[3] H. J. Jia, X. M. Li, Y. F. Mu, et al. Coordinated control for EV aggregators and power plants in frequency regulation considering time-varying delays[J]. Applied Energy, 2018, 210(15): 1363-1376.

[4] C. Y. Dong, S. F. Yang, and H. J. Jia. Padé-based stability analysis for modular multilevel converter considering the time delay in the digital control system[J]. IEEE Transactions on Industrial Electronics, 2018, 66(7): 5242 - 5253.

[5] L. Jiang, W. Yao, Q. H. Wu, et al. Delay-Dependent Stability for Load Frequency Control With Constant and Time-Varying Delays[J]. IEEE Transactions on Power Systems, 2012, 27(2): 932-941.

[6] X. F. Yu, K. Tomsovic. Application of linear matrix inequalities for load frequency control with communication delays[J]. IEEE Transactions on Power Systems, 2004, 19(3): 1508-1515.